*Published online 24 March 2022* *Nucleic Acids Research, 2022, Vol. 50, Web Server issue* ***W175–W182***
*https://doi.org/10.1093/nar/gkac199*

# ChIP-Atlas 2021 update: a data-mining suite for exploring epigenomic landscapes by fully integrating ChIP-seq, ATAC-seq and Bisulfite-seq data

**Zhaonan Zou[1,2,3], Tazro Ohta[4], Fumihito Miura[5] and Shinya Oki[1,6,*]**

[1]Department of Drug Discovery Medicine, Kyoto University Graduate School of Medicine, 53 Shogoin Kawahara-cho, Sakyo-ku, Kyoto 606-8507, Japan, [2]Kyoto University Graduate Program for Medical Innovation, Yoshida-Konoe-cho, Sakyo-ku, Kyoto 606-8501, Japan, [3]Kyoto University Graduate Division, Yoshida-Nihonmatsu-cho, Sakyo-ku, Kyoto 606-8501, Japan, [4]Database Center for Life Science, Joint Support-Center for Data Science Research, Research Organization of Information and Systems, Yata 1111, Mishima, Shizuoka 411-8540, Japan, [5]Department of Biochemistry, Kyushu University Graduate School of Medical Sciences, 3-1-1 Maidashi, Higashi-ku, Fukuoka 812-8582, Japan and [6]Precursory Research for Embryonic Science and Technology, Japan Science and Technology Agency, 4-1-8 Honcho, Kawaguchi, Saitama 332-0012, Japan

Received January 11, 2022; Revised February 21, 2022; Editorial Decision March 11, 2022; Accepted March 22, 2022

## ABSTRACT

**ChIP-Atlas (https://chip-atlas.org) is a web service providing both GUI- and API-based data-mining tools to reveal the architecture of the transcription regulatory landscape. ChIP-Atlas is powered by comprehensively integrating all data sets from high-throughput ChIP-seq and DNase-seq, a method for profiling chromatin regions accessible to DNase. In this update, we further collected all the ATAC-seq and whole-genome bisulfite-seq data for six model organisms (human, mouse, rat, fruit fly, nematode, and budding yeast) with the latest genome assemblies. These together with ChIP-seq data can be visualized with the Peak Browser tool and a genome browser to explore the epigenomic landscape of a query genomic locus, such as its chromatin accessibility, DNA methylation status, and protein–genome interactions. This epigenomic landscape can also be characterized for multiple genes and genomic loci by querying with the Enrichment Analysis tool, which, for example, revealed that inflammatory bowel disease-associated SNPs are the most significantly hypo-methylated in neutrophils. Therefore, ChIP-Atlas provides a panoramic view of the whole epigenomic landscape. All datasets are free to download via either a simple button on the web page or an API.**

## GRAPHICAL ABSTRACT

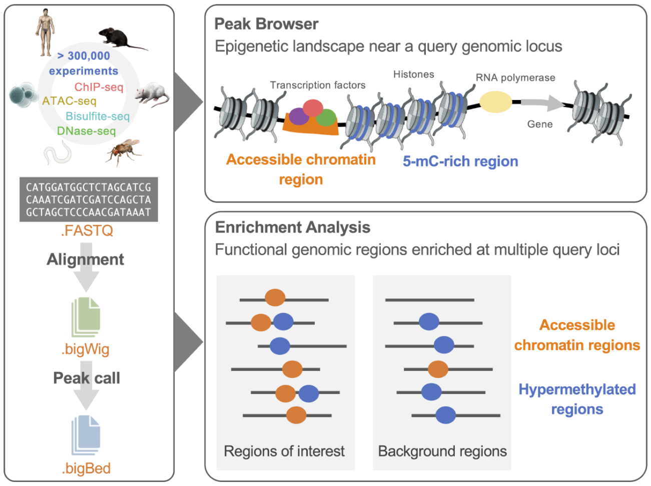

## INTRODUCTION

In the past decade, despite the increasing number of high-throughput sequencing experiments, the secondary use of the obtained raw data has required complex and large-scale computational processing, and thus most data are still being hoarded. Since 2015, we have been comprehensively collecting, analyzing and integrating almost all chromatin immunoprecipitation sequencing (ChIP-seq) (1) and DNase-seq (2)—a method for profiling chromatin regions accessible to DNase—data derived from six representative model organisms (*Homo sapiens*, *Mus musculus*, *Rattus norvegicus*, *Drosophila melanogaster*, *Caenorhabditis elegans* and *Saccharomyces cerevisiae*) archived at the Sequence Read Archive (SRA). SRA is the largest publicly available data

[*]To whom correspondence should be addressed. Tel: +81 75 366 7479; Email: oki.shinya.3w@kyoto-u.ac.jp

repository that accepts submissions of high-throughput sequencing data, which is maintained by NCBI, EBI, and DDBJ. Data-mining tools powered by these data were provided through our web server, ChIP-Atlas (https://chip-atlas.org) (3), for visualization of assembled peak data and enrichment analysis for given genomic loci to identify transcription factor (TF) binding and histone modification status. ChIP-Atlas is powered by dedicated manual curation and annotation of experimental metadata, and a uniform data process pipeline to reveal the complex architecture of the transcription regulatory landscape.

Information on TF binding and histone marks is, however, still insufficient to fully understand the regulatory systems for gene expression control because an absence of nucleosomes and low methylation levels also characterize active promoters, enhancers, and other gene regulatory sequences (4–7). To detect accessible chromatin regions, several experimental methods including DNase-seq, formaldehyde-assisted isolation of regulatory elements (8), and assay for transposase-accessible chromatin with sequencing (ATAC-seq) (9) have been developed. Among these, ATAC-seq identifies accessible chromatin regions based on their increased accessibility to Tn5 transposase integration and is now predominantly used given its advantages of technical ease and sensitivity to a small number of cells. In contrast, bisulfite sequencing (Bisulfite-seq) is a well-established protocol to detect methylated cytosines in genomic DNA, which employs a chemical method that selectively deaminates unmodified cytosine to uracil while leaving 5-methylcytosine intact before DNA sequencing (10).

Here, we describe the ChIP-Atlas 2021 update, which collected all the ATAC-seq ($n$ = 66 104) and whole-genome bisulfite sequencing (WGBS) data ($n$ = 51 074) for the six representative model organisms. This update makes ChIP-Atlas, to our knowledge, the first and only web service that enables users to explore not only protein binding, but also chromatin accessibility and DNA methylation status, within a single given genomic region of interest (ROI) at the same time (Peak Browser tool). ChIP-Atlas can also be used to reveal the regulatory network involved in a batch of genomic ROIs (Enrichment Analysis tool) based on ATAC-seq and WGBS data in addition to ChIP-seq data in the previous version. ChIP-Atlas provides a panoramic view of the whole epigenomic landscape and should be of great interest to researchers in the fields of genetics and genomics, as well as those studying transcriptional regulation in general.

## MATERIALS AND METHODS

### Source data obtained from SRA

We obtained sample metadata from the NCBI BioSample database FTP server (ftp://ftp.ncbi.nlm.nih.gov/biosample). We also retrieved the metadata of SRA experiments (accession number with the prefix SRX, ERX or DRX; hereafter SRXs), such as library preparation or used sequencing instrument models, from the NCBI SRA FTP server (ftp://ftp.ncbi.nlm.nih.gov/sra/reports/Metadata). ChIP-Atlas uses ATAC-seq and WGBS SRXs that meet the following criteria: LIBRARY_STRATEGY is 'ATAC-seq' or 'Bisulfite-seq'; LIBRARY_SOURCE is 'GENOMIC'; LIBRARY_SELECTION is 'PCR' or 'others' for ATAC-seq, and 'RANDOM' for WGBS; taxonomy_name is '*Homo sapiens,*' '*Mus musculus*', '*Rattus norvegicus*', '*Caenorhabditis elegans*', '*Drosophila melanogaster*' or '*Saccharomyces cerevisiae*'; and INSTRUMENT_MODEL includes 'Illumina', 'NextSeq' or 'HiSeq.' For ChIP-seq and DNase-seq data, refer to the previous paper on ChIP-Atlas (3).

### Primary processing

Binarized sequence raw data (.sra) for each SRX were downloaded and decompressed into FASTQ format with the 'fasterq-dump' command of SRA Toolkit (ver. 2.9.4; https://ftp-trace.ncbi.nlm.nih.gov/sra/sdk/2.9.4/sratoolkit.2.9.4-ubuntu64.tar.gz) according to the default mode, with the exception of paired-end reads, which were decoded with the '-split-files' option. For ATAC-seq data, the subsequent alignment (with Bowtie2 [ver. 2.2.2] (11)) and peak call (with MACS2 [ver. 2.1.1; macs2 callpeak] (12)) process was the same as that for ChIP-seq and DNase-seq data, which was previously described in the first ChIP-Atlas paper. As for WGBS data, BMap (ver. 1.0; https://github.com/FumihitoMiura/Project-2/blob/master/Project-2.tar.gz) (13), a speedy aligner with small temporary file sizes, was used for alignment and MethPipe (ver. 4.1.1; https://github.com/smithlabcode/methpipe/releases/download/v4.1.1/methpipe-4.1.1.tar.gz) (14) was subsequently used as a region-caller for identifying hyper-, partially and hypo-methylated regions (MRs). After creation of the index files for all genome assemblies, we aligned the downloaded FASTQ files against the reference genomes with the '-fastq' and '-pfastq' options for single-end and paired-end reads, respectively. The alignment data (in bigWig format) containing methylation level and coverage information were generated for each SRX. Methylation level and coverage were then calculated for each CpG, and these data were next streamed into MethPipe. The 'hypermr,' 'pmd,' and 'hmr' sub-commands of MethPipe were used for identifying hyper-, partially, and hypo-MRs (in bigBed format), respectively, for each SRX according to the default mode.

### Analysis of disease-associated SNPs

GWAS SNP data were downloaded from the website of UCSC genome browser (https://hgdownload.soe.ucsc.edu/goldenPath/hg19/database/gwasCatalog.txt.gz; on 21 December 2021) (15). A BED format file was created by extending the genomic coordinates of all SNPs by 5 kb up- and downstream. Genomic regions containing SNPs were then categorized into 'inflammatory bowel disease (IBD)-associated' ($n$ = 393) and 'Others' ($n$ = 189 036) according to the disease/phenotype names listed in the 'trait' column. The IBD-associated SNPs (in BED format) were directly used as 'dataset A' for the Enrichment Analysis tool on the ChIP-Atlas web interface. Meanwhile, 3930 SNPs in the 'Others' category, which is ten times the number of IBD-associated SNPs, were randomly selected as the background data for 'dataset B'.

## RESULTS

### Overview of the ChIP-Atlas update

In this update, the major expansion of the experiment types results in significant growth in the number of experiments and the number of annotated functional genome regions by including all ATAC-seq and WGBS datasets archived at SRA (Figure 1A, Table 1). For unified management of the records, each experiment is assigned a unique ID (hereafter referred to as 'SRX') in ChIP-Atlas, which is exactly the same as the original SRA accession number. The number of SRXs collected in ChIP-Atlas is over 300 000 for the six organisms, which corresponds to 84.3% of the total number of ChIP-seq, ATAC-seq, DNase-seq and Bisulfite-seq SRXs in SRA for all of these organisms ($n$ = 362 121 as of September 2021; Table 1). In this update, we adopted the latest version of genome assemblies in addition to previous ones (Table 2). Since the public release of ChIP-Atlas, the data have been updated monthly concurrent with the monthly update of the NCBI SRA metadata dump (Figure 1B), by which >100 000 ChIP-seq experimental datasets have been added since 2018 (Table 1).

We manually curated and annotated the cell types used in each experiment according to commonly or officially adopted nomenclature. The cell types were further categorized into superordinate 'cell type classes' (Figure 1C). We adapted a uniformed data process pipeline (Figure 1D; detailed in the Materials and Methods), in which the ChIP-seq, ATAC-seq, and DNase-seq data are aligned to corresponding reference genomes with Bowtie2 (11) and then subjected to peak calling with MACS2 (12); meanwhile, for WGBS data, we align the raw reads against the reference genomes using BMap before applying MethPipe for statistically calling hyper-, partially, and hypo-methylated regions (MRs). All alignment and peak-call data are freely downloadable from http://dbarchive.biosciencedbc.jp/kyushu-u/ (detailed on the documentation page of ChIP-Atlas [https://github.com/inutano/chip-atlas/wiki/#downloads_doc]), and can be browsed by users in the IGV genome browser (16) by entering the SRX ID or a given keyword (or keywords) in the corresponding Data Search page of ChIP-Atlas (Supplementary Figure S1 and Supplementary Material S1).

### Example of use

*Peak browser.* All peak-call data recorded in ChIP-Atlas can be presented graphically with the Peak Browser tool. One can therefore easily understand not only protein–genome interactions (ChIP-seq), but also chromatin accessibility (ATAC-seq) and DNA methylation levels (WGBS), within any query genomic region of interest (ROI). To implement this tool, we integrated a large amount of peak-call data, indexed them for IGV, and constructed a web interface that externally controls IGV preinstalled on the user's machine (tested on Mac, Windows and Linux platforms). For instance, upon the specification of ChIP-seq, ATAC-seq or WGBS data of mouse spermatogonia on the web page (Figure 2A), the corresponding results are automatically streamed into IGV (Figure 2B). In this case, multiple ATAC-seq and WGBS in spermatogonia data characterize an accessible chromatin region and hypo-MR, respectively, at the locus between the *Tcf19* and *Cchcr1* genes, where multiple factors such as Smarca4, Zbtb16, and Sall4 are colocalized, suggesting that the *Tcf19–Cchcr1* locus is robustly hypo-methylated and open to bind Sall4 and other TFs in spermatogonia. Representative ChIP-seq (SRX1284250), ATAC-seq (SRX5884282) and WGBS (SRX749893) alignment data are also exhibited in the top panel of Figure 2B. The IGV sessions can be saved as XML files at any moment, so that the results obtained by using the Peak Browser tool can be easily and precisely shared among collaborators (Supplementary Material S2). With the use of ChIP-Atlas, users can not only check individual experimental data, but also browse an integrative landscape of multiple epigenetic profiling results, potentially providing useful insight into the location of functional genomic regions (enhancers, promoters and insulators) and the corresponding regulators.

*Enrichment analysis.* Enrichment Analysis is a tool that allows a search for TFs, accessible chromatin regions, and hypo- or hyper-MRs enriched at a batch of genomic ROIs or gene loci. Upon the submission of two sets of genomic regions (ROIs and background regions), all SRXs are evaluated to count the overlaps between the peaks and submitted regions and to perform Fisher's exact test, before returning the enrichment analysis results in HTML and TSV formats. Although ChIP-Atlas can generate random background regions for comparison to ROIs, the users are strongly recommended to provide biologically appropriate background genomic intervals because most randomly selected regions are probabilistically devoid of any functional genomic annotation. The results are assigned unique URLs, which are permanently available to the public. As an example of usage, we selected inflammatory bowel disease (IBD)-associated SNPs identified by GWAS as the ROIs ($n$ = 393) and other SNPs as the background ($n$ = 3930), and we applied these selections to the Enrichment Analysis tool (Figure 2C; detailed in the Materials and Methods). The results in HTML format are shown in Figure 2D (upper), including SRX IDs (column 1), features (column 3), cell types (column 5), $P$-values (column 9) and fold enrichments (column 11), where hypo-MRs of neutrophils are significantly enriched ($P = 1 \times 10^{-17}$). To visually interpret the results, we downloaded the resultant TSV files (refer to Supplementary Table S1 for unique URLs for each analysis) and generated volcano plots (Figure 2D [bottom]; Supplementary Table S1). The IBD-associated SNPs were shown to be enriched in hypo-MRs and accessible chromatin regions of blood-related cells (red in Figure 2D), including the ATAC-seq peaks of macrophages ($P = 1 \times 10^{-20}$) and Th17 cells ($P = 1 \times 10^{-17}$), both involved in the inflammation of IBD. Furthermore, the enrichment analysis of TF ChIP-seq data revealed that the IBD-associated SNPs were preferentially bound by STAT1 in monocytes ($P = 1 \times 10^{-22}$) and SPI1 in macrophages ($P = 1 \times 10^{-21}$), essential factors for inflammation and macrophage differentiation, respectively, which is consistent with the nature of IBD as an autoimmune disease (17). All resultant URLs for generating Figure 2D are summarized in Supplementary Table S2. API of the Enrichment Analysis tool is also provided by ChIP-Atlas, the general

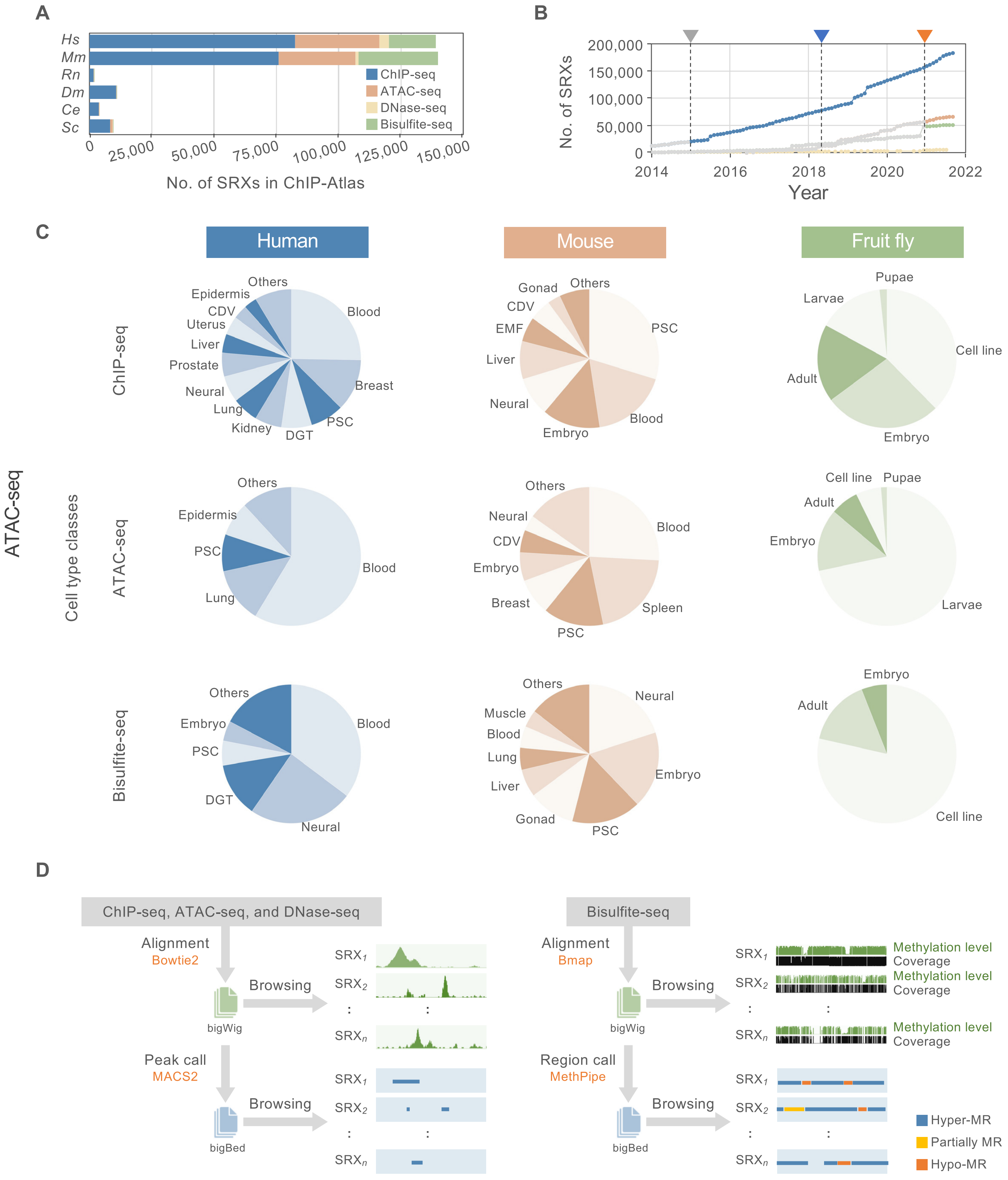

**Figure 1.** Overview of the ChIP-Atlas data set and computational processing. (**A**) Numbers of ChIP-seq, DNase-seq, ATAC-seq and WGBS experiments recorded in ChIP-Atlas (as of September 2021). Colors indicate different experiment types. Color legend is shown in the figure. *Hm, Homo sapiens; Mm, Mus musculus; Rn, Rattus norvegicus; Dm, Drosophila melanogaster; Ce, Caenorhabditis elegans; Sc, Saccharomyces cerevisiae*. (**B**) Cumulative number of SRX-based experiments recorded in ChIP-Atlas. Colors of the dots indicate different experiment types. Color legend is the same as that in (A). The gray, blue, and orange arrowheads indicate the timing of the release of ChIP-Atlas in 2015, the publication of the first ChIP-Atlas paper in 2018, and the inclusion of ATAC-seq and WGBS in 2021, respectively. ChIP-seq and DNase-seq data published before 2015, and ATAC-seq or WGBS data published before January 2021 are shown in gray. (**C**) Numbers of experiments according to cell type classes for human, mouse, and fruit fly data. PSC, pluripotent stem cell; CDV, cardiovascular; DGT, digestive tract; EMF, embryonic fibroblast. (**D**) Overview of data processing. Raw sequence data are downloaded from NCBI SRA, aligned to a reference genome, and subjected to peak calling, all of which can be monitored with the IGV genome browser. MR, methylated region.

**Table 1.** Data statistics of ChIP-Atlas

| Experiment type | ChIP-seq | | ATAC-seq | DNase-seq | Bisulfite-seq | All |
|---|---|---|---|---|---|---|
| Year | 2021 | 2018 | 2021 | 2021 | 2021 | 2021 |
| Number of experiments | 182 891 | 74 076 | 66 104 | 5346 | 51 074 | 305 415 |
| Number of ChIP antigens | 2 477 | 1 979 | NA | NA | NA | 2 477 |
| Number of cell types | 2 486 | 1 615 | 772 | 406 | 553 | 2 918 |
| Number of peaks | 1 329 049 688 | 717 206 934 | 362 032 813 | 128 597 931 | 3 798 954 139 | 5 618 634 571 |

**Table 2.** Comparison of ChIP-Atlas with other similar web services

| | ChIP-Atlas | Cistrom DB | ReMap | GTRD | MethBank |
|---|---|---|---|---|---|
| Data source | NCBI SRA | GEO, ENCODE, and Roadmap Epigenetics | GEO, ENCODE, and ENA | GEO, SRA, ENCODE, and modENCODE | NCBI SRA and Genome Sequence Archive |
| Experiments | ChIP-seq, **ATAC-seq**, DNase-seq, and **Bisulfite-seq** | ChIP-seq, ATAC-seq, and DNase-seq | ChIP-seq, ChIP-exo, and DAP-seq | ChIP-seq, ChIP-exo, ChIP-nexus, MNase-seq, DNase-seq, FAIRE-seq, ATAC-seq, and RNA-seq | Bisulfite-seq |
| Filtering of data for quality control | No | Yes | Yes | No | Yes |
| Number of experiments | 76 217 → **305 415** | 56 442 | 19 983 | 36 540 | 673 |
| Organism | Hs, Mm, Rn, Dm, Ce, and Sc | Hs and Mm | Hs, Mm, Dm and At | Hs, Mm, At, Ce, Dr, Dm, Rn, Sc and Sp | Hs, Dr, Mm, Os, Gm, Me, Pv and Sl |
| Genome assembly | hg19, **hg38**, mm9, **mm10**, rn6, dm3, **dm6**, ce10, **ce11** and sacCer3 | hg38 and mm10 | hg38, mm10, dm6, and tair10 (can be lifted to hg19/mm9 with liftover) | hg38, mm10, tair10, ce11, danRer11, dm6, rn6, sacCer3 and spo2 | hg38, danRer7, mm10, IRGSP-1.0, Gmax_275_v2.0, Mesculenta_305_v6, Pvulgaris_218_v1 and GCF_000188115.3_SL2.53 |
| Alignment tool | Bowtie2/**BMap** | BWA | Bowtie2 | Bowtie2 | WSBA |
| Peak caller | MACS2/**MethPipe** | MACS2 | MACS2 | MACS2, MACS, GEM, PICS, SISSRs | NA |
| Display format for each experiment | Alignment and peaks | Alignment and peaks | Peaks | Peaks | Alignment |
| Browsing assembled peaks | Possible | None | Possible | Possible | NA |
| Genome browser | IGV and UCSC | WashU and UCSC | UCSC, ENSEMBL and IGV | Self-developed, UCSC and ENSEMBL | JBrowse |
| Integrative analysis tools | Search tool for target genes and colocalizing factors of given TF, and enrichment analysis tool for given genes and genomic coordinates | Search tool for target genes of single experiment, TFs binding to single given genomic locus or query gene | Enrichment analysis tool for given genomic coordinates relative to random background | Search tool for target genes of given TF | Predictor of DNA methylation, age of human blood and enrichment analysis tool for identification of differentially methylated promoters |

*Hm*, *Homo sapiens*; *Mm*, *Mus musculus*; *Rn*, *Rattus norvegicus*; *Dm*, *Drosophila melanogaster*; *Ce*, *Caenorhabditis elegans*; *Sc*, *Saccharomyces cerevisiae*; *At*, *Arabidopsis thaliana*; *Dr*, *Danio rerio*; *Sp*, *Schizosaccharomyces pombe*; *Os*, *Oryza sativa*; *Gm*, *Glycine max*; *Me*, *Manihot esculenta*; *Pv*, *Phaseolus vulgaris*; *Sl*, *Solanum lycopersicum*.

instructions for which can be found on the documentation page (https://github.com/inutano/chip-atlas/wiki/Perform-Enrichment-Analysis-programmatically).

## DISCUSSION

In this paper, we present a major update of ChIP-Atlas involving significant expansion in the number of experiments by including all public ATAC-seq and WGBS data. The updated web service enables users to explore not only protein binding, but also chromatin accessibility and DNA methylation levels within single (Peak Browser tool) or multiple (Enrichment Analysis tool) queries of genomic ROIs or gene loci. As an example of use, we performed enrichment analysis to reveal that IBD-associated SNPs are the most significantly hypo-methylated in the neutrophils, a granu-

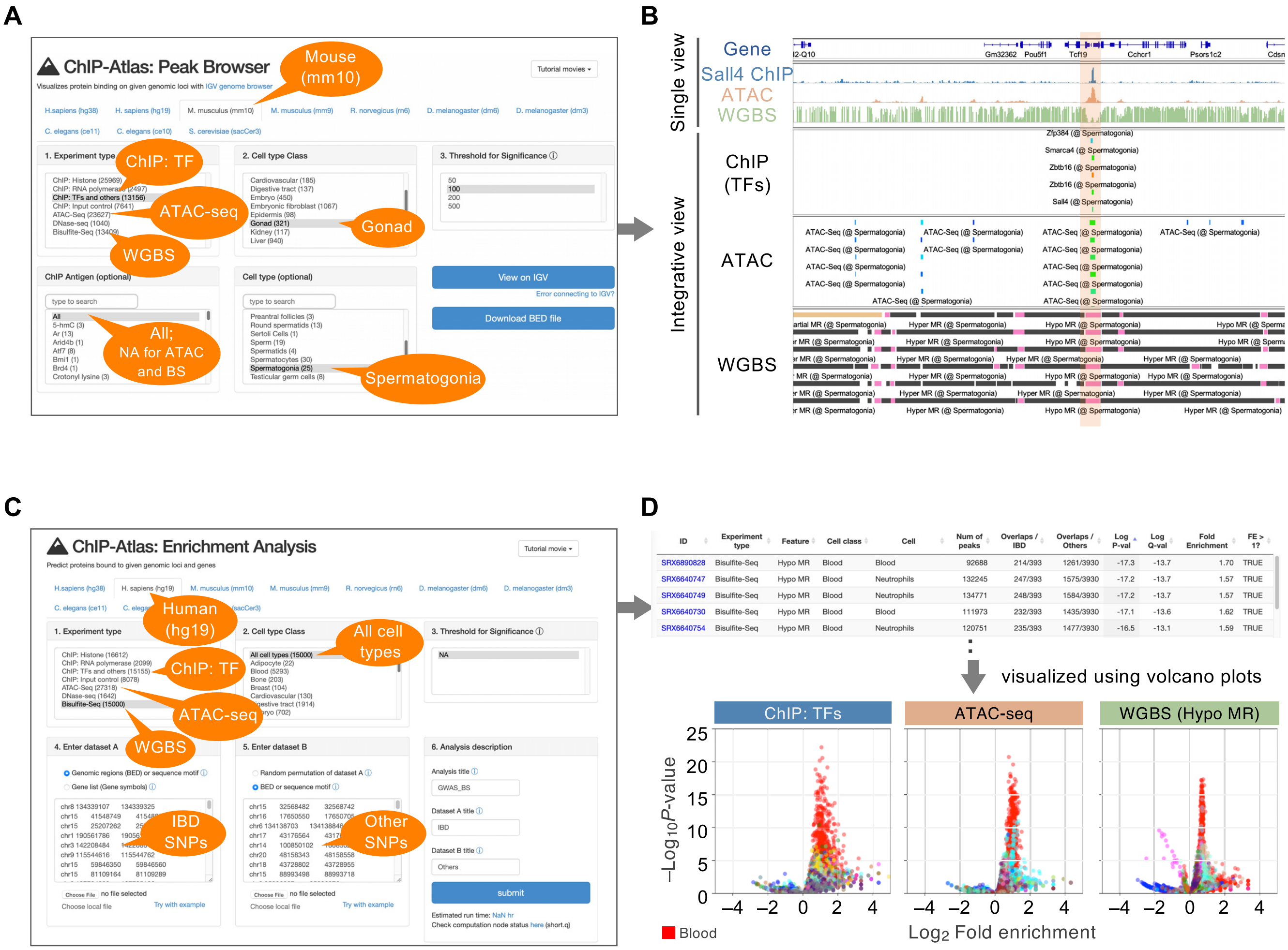

ChIP-Atlas: Peak Browser

Visualizes protein binding on given genomic loci with IGV genome browser

Tutorial movies

H.sapiens (hg38) | H. sapiens (hg19) | M. musculus (mm10) | M. musculus (mm9) | R. norvegicus (rn6) | D. melanogaster (dm6) | D. melanogaster (dm3) | C. elegans (ce11) | C. elegans (ce10) | S. cerevisiae (sacCer3)

1. Experiment type

ChIP: Histone (25969)
ChIP: RNA polymerase (2497)
ChIP: TFs and others (13156)
ChIP: Input control (7641)
ATAC-Seq (23627)
DNase-seq (1040)
Bisulfite-Seq (13409)

2. Cell type Class

Cardiovascular (185)
Digestive tract (137)
Embryo (450)
Embryonic fibroblast (1067)
Epidermis (98)
Gonad (321)
Kidney (117)
Liver (940)

3. Threshold for Significance ⓘ

50
100
200
500

ChIP Antigen (optional)

type to search

All
5-hmC (3)
Ar (13)
Arid4b (1)
Atf7 (8)
Bmi1 (1)
Brd4 (1)
Crotonyl lysine (3)

Cell type (optional)

type to search

Preantral follicles (3)
Round spermatids (13)
Sertoli Cells (1)
Sperm (19)
Spermatids (4)
Spermatocytes (30)
Spermatogonia (25)
Testicular germ cells (8)

View on IGV

Error connecting to IGV?

Download BED file

ChIP-Atlas: Enrichment Analysis

Predict proteins bound to given genomic loci and genes

Tutorial movie

H.sapiens (hg38) | H. sapiens (hg19) | M. musculus (mm10) | M. musculus (mm9) | R. norvegicus (rn6) | D. melanogaster (dm6) | D. melanogaster (dm3) | C. elegans (ce11) | C. elega | (sacCer3)

1. Experiment type

ChIP: Histone (16612)
ChIP: RNA polymerase (2099)
ChIP: TFs and others (15155)
ChIP: Input control (8078)
ATAC-Seq (27318)
DNase-seq (1642)
Bisulfite-Seq (15000)

2. Cell type Class

All cell types (15000)
Adipocyte (22)
Blood (5293)
Bone (203)
Breast (104)
Cardiovascular (130)
igestive tract (1914)
ryo (702)

3. Threshold for Significance ⓘ

NA

4. Enter dataset A

● Genomic regions (BED) or sequence motif ⓘ
○ Gene list (Gene symbols) ⓘ

```
chr8 134339107    134339325
chr15     41548749     4154
chr15     25207262     25
chr1 190561786    19056
chr3 142208484
chr9 115544616    115544762
chr15     59846350     59846560
chr15     81109164     81109289
```

Choose File no file selected
Choose local file     Try with example

5. Enter dataset B

○ Random permutation of dataset A ⓘ
● BED or sequence motif ⓘ

```
chr15     32568482     32568742
chr16     17650550     17650705
chr6 134138703    134138846
chr17     43176564     4317
chr14     100850102
chr20     48158343     48158558
chr18     43728802     43728955
chr15     88993498     88993718
```

Choose File no file selected
Choose local file     Try with example

6. Analysis description

Analysis title ⓘ: GWAS_BS

Dataset A title ⓘ: IBD

Dataset B title ⓘ: Others

submit

Estimated run time: NaN hr
Check computation node status here (short.q)

| ID | Experiment type | Feature | Cell class | Cell | Num of peaks | Overlaps / IBD | Overlaps / Others | Log P-val | Log Q-val | Fold Enrichment | FE > 1? |
|---|---|---|---|---|---|---|---|---|---|---|---|
| SRX6890828 | Bisulfite-Seq | Hypo MR | Blood | Blood | 92688 | 214/393 | 1261/3930 | -17.3 | -13.7 | 1.70 | TRUE |
| SRX6640747 | Bisulfite-Seq | Hypo MR | Blood | Neutrophils | 132245 | 247/393 | 1575/3930 | -17.2 | -13.7 | 1.57 | TRUE |
| SRX6640749 | Bisulfite-Seq | Hypo MR | Blood | Neutrophils | 134771 | 248/393 | 1584/3930 | -17.2 | -13.7 | 1.57 | TRUE |
| SRX6640730 | Bisulfite-Seq | Hypo MR | Blood | Blood | 111973 | 232/393 | 1435/3930 | -17.1 | -13.6 | 1.62 | TRUE |
| SRX6640754 | Bisulfite-Seq | Hypo MR | Blood | Neutrophils | 120751 | 235/393 | 1477/3930 | -16.5 | -13.1 | 1.59 | TRUE |

**Figure 2.** Examples of use of the integrative analysis tools in ChIP-Atlas. (**A**) Parameters when users perform a query to show chromatin accessibility, methylation status, and TF binding around mouse *Tcf19–Cchcr1* locus in spermatogonia using the Peak Browser tool. (**B**) Peak-call data for TF ChIP-seq, ATAC-seq and WGBS SRXs around the mouse *Tcf19–Cchcr1* locus are shown in the IGV genome browser. The highlighted region indicates an accessible chromatin and hypo-methylated region. Bars represent the peak regions, with the curated names of the ChIP antigens (only for ChIP-seq peaks) and cell types being shown below the bars. The color of the bars in the 'ChIP (TFs)' and 'ATAC' panel indicates the score calculated with the peak-caller MACS2 ($-\log_{10}$[$Q$-value]). Black, pink, and beige bars in the 'WGBS' panel indicate hyper-, hypo- and partially methylated regions, respectively. (**C**) Parameters when users perform a query to evaluate TF binding, chromatin accessibility, and methylation levels of multiple IBD-associated SNPs in all cell types. (**D**) The resultant HTML of enrichment analysis using WGBS data (upper). Volcano plots for visualizing the results (bottom). X-axis, $\log_2$[fold enrichment]; Y-axis, $-\log_{10}$[$P$-value]. Each dot represents an individual SRX. SRXs are categorized by cell type classes and indicated by different colors. Red, 'Blood' class. The whole color legend is summarized in Supplementary Table S2.

locyte subtype known to be involved in autoinflammatory IBD (17).

Before and after the public release of ChIP-Atlas, several similar web services have been released (Table 2). For ChIP-seq, ATAC-seq and DNase-seq data, Cistrome DB (http://cistrome.org/db/), ReMap (https://remap2022.univ-amu.fr/), and GTRD (https://gtrd.biouml.org/) are representatives providing thousands of preprocessed datasets (18–20). As for Bisulfite-seq data, MethBank (http://bigd.big.ac.cn/methbank) is widely used (21). ChIP-Atlas covers much more experimental data than all of these other services. ChIP-Atlas does not cover ChIP-exo (22) and MNase-seq (23) data, in contrast to ReMap and GTRD, and there are fewer available organisms than in GTRD and MethBank. Alignment data (in bigWig format) are available from ChIP-Atlas, Cistrome DB and MethBank. Integrative analysis tools are provided in all services. Enrichment analysis is possible with ChIP-Atlas in both a GUI and an API, while ReMap provides such a tool in a CLI (R package named 'ReMapEnrich'). Since the publication of the first ChIP-Atlas paper, we have improved the service to make it compatible with the latest versions of reference genomes such as hg38 for human and mm10 for mouse, as is the case for other services. Meanwhile, alignment of raw reads against old references is still performed during the monthly update of ChIP-Atlas, and alignment and peak-call data in old versions are still provided for analyzing the data of users obtained years ago.

In addition to the examples of use mentioned in the RESULTS section, ChIP-Atlas has been cited by hundreds of peer-reviewed articles since its first release in 2015, including research for analyzing cis-regulatory elements of certain genes (24,25), and TF enrichment at genomic ROIs and query genes (26–30) (see http://chip-atlas.org/publications for the full list of publications citing ChIP-Atlas). Furthermore, because all alignment (bigWig) and peak-call (bigBed) data can be freely downloaded, ChIP-Atlas is now interconnecting with many other databases or web services such as UCSC Browser, DeepBlue (an epigenomic data server providing a central data access hub for large collections of epigenomic data), RegulatorTrail (a web service predicting target genes of TFs), jPOSTrepo (a data repository of sharing raw/processed mass spectrometry data), and the Signaling Pathways Project (a multi-omics knowledgemine based upon public transcriptomic and cistromic datasets) (31–35). Along with the inclusion of ATAC-seq and WGBS data, and the ongoing monthly updates with semiautomatic pipelines and systematic curation, the source data in ChIP-Atlas are continuously expanding. We are planning to include more experiment types such as CUT&Tag (36) and ChIL-seq (37) and more organisms including plants such as *Arabidopsis thaliana*. Integration of preprocessed 3D genome conformation data such as Hi-C datasets (38) into the Peak Browser and Enrichment Analysis tool is also on the agenda.

## DATA AVAILABILITY

ChIP-Atlas (https://chip-atlas.org) is a publicly available web server with no sign up required. Documentation for data processing and downloadable data are available in the 'Documentation' section (https://github.com/inutano/chip-atlas/wiki).

## SUPPLEMENTARY DATA

Supplementary Data are available at NAR Online.

## ACKNOWLEDGEMENTS

The website of ChIP-Atlas is hosted on a server provided by the National Bioscience Database Center, Japan. Computations were mostly performed on the NIG supercomputer at ROIS National Institute of Genetics. We thank Prof. Shuh Narumiya and members of the Department of Drug Discovery Medicine at Kyoto University Graduate School of Medicine. We also thank Edanz (https://jp.edanz.com/ac) for editing a draft of this manuscript. The images used in the Graphical Abstract are from TogoTV (© 2016 DBCLS TogoTV).

## FUNDING

KAKENHI grants [16H06530 to Z.Z. and S.O., 18KT0024 and 19H03424 to S.O.] from the Ministry of Education, Culture, Sports, Science, and Technology of Japan; MIP Interdisciplinary Joint Research grant from Kyoto University (to Z.Z.); SPRING [JPMJSP2110 to Z.Z.], NBDC (to S.O.), ERATO [JPMJER2101 to S.O.] and PRESTO [JPMJPR1942 to S.O.] from the Japan Science and Technology Agency, and Japan Agency for Medical Research and Development [JP20gm5010003 to S.O.]. Funding for open access charge: NBDC.

*Conflict of interest statement.* None declared.

## REFERENCES

1. Johnson,D.S., Mortazavi,A., Myers,R.M. and Wold,B. (2007) Genome-wide mapping of in vivo protein-DNA interactions. *Science*, **316**, 1497–1502.
2. Boyle,A.P., Davis,S., Shulha,H.P., Meltzer,P., Margulies,E.H., Weng,Z., Furey,T.S. and Crawford,G.E. (2008) High-resolution mapping and characterization of open chromatin across the genome. *Cell*, **132**, 311–322.
3. Oki,S., Ohta,T., Shioi,G., Hatanaka,H., Ogasawara,O., Okuda,Y., Kawaji,H., Nakaki,R., Sese,J. and Meno,C. (2018) ChIP-Atlas: a data-mining suite powered by full integration of public chip-seq data. *EMBO Rep.*, **19**, e46255.
4. Bird,A. (2002) DNA methylation patterns and epigenetic memory. *Genes Dev.*, **16**, 6–21.
5. Cedar,H. and Bergman,Y. (2012) Programming of DNA methylation patterns. *Annu. Rev. Biochem.*, **81**, 97–117.
6. Owen-Hughes,T. and Gkikopoulos,T. (2012) Making sense of transcribing chromatin. *Curr. Opin. Cell Biol.*, **24**, 296–304.
7. Li,B., Carey,M. and Workman,J.L. (2007) The role of chromatin during transcription. *Cell*, **128**, 707–719.
8. Giresi,P.G., Kim,J., McDaniell,R.M., Iyer,V.R. and Lieb,J.D. (2007) FAIRE (formaldehyde-assisted isolation of regulatory elements) isolates active regulatory elements from human chromatin. *Genome Res.*, **17**, 877–885.
9. Buenrostro,J.D., Giresi,P.G., Zaba,L.C., Chang,H.Y. and Greenleaf,W.J. (2013) Transposition of native chromatin for fast and sensitive epigenomic profiling of open chromatin, DNA-binding proteins and nucleosome position. *Nat. Methods*, **10**, 1213–1218.
10. Frommer,M., McDonald,L.E., Millar,D.S., Collis,C.M., Watt,F., Grigg,G.W., Molloy,P.L. and Paul,C.L. (1992) A genomic sequencing protocol that yields a positive display of 5-methylcytosine residues in individual DNA strands. *Proc. Nat. Acad. Sci. U.S.A.*, **89**, 1827–1831.
11. Langmead,B. and Salzberg,S.L. (2012) Fast gapped-read alignment with Bowtie 2. *Nat. Methods*, **9**, 357–359.
12. Zhang,Y., Liu,T., Meyer,C.A., Eeckhoute,J., Johnson,D.S., Bernstein,B.E., Nussbaum,C., Myers,R.M., Brown,M., Li,W. *et al.* (2008) Model-based analysis of chip-Seq (MACS). *Genome Biol.*, **9**, R137.
13. Miura,F., Enomoto,Y., Dairiki,R. and Ito,T. (2012) Amplification-free whole-genome bisulfite sequencing by post-bisulfite adaptor tagging. *Nucleic Acids Res.*, **40**, e136.
14. Song,Q., Decato,B., Hong,E.E., Zhou,M., Fang,F., Qu,J., Garvin,T., Kessler,M., Zhou,J. and Smith,A.D. (2013) A reference methylome database and analysis pipeline to facilitate integrative and comparative epigenomics. *PLoS One*, **8**, e81148.
15. Navarro Gonzalez,J., Zweig,A.S., Speir,M.L., Schmelter,D., Rosenbloom,K.R., Raney,B.J., Powell,C.C., Nassar,L.R., Maulding,N.D., Lee,C.M. *et al.* (2021) The UCSC genome browser database: 2021 update. *Nucleic Acids Res.*, **49**, D1046–D1057.
16. Thorvaldsdóttir,H., Robinson,J.T. and Mesirov,J.P. (2013) Integrative genomics viewer (IGV): high-performance genomics data visualization and exploration. *Brief. Bioinf.*, **14**, 178–192.
17. Chang,J.T. (2020) Pathophysiology of inflammatory bowel diseases. *N. Engl. J. Med.*, **383**, 2652–2664.
18. Zheng,R., Wan,C., Mei,S., Qin,Q., Wu,Q., Sun,H., Chen,C.H., Brown,M., Zhang,X., Meyer,C.A. *et al.* (2019) Cistrome data browser: expanded datasets and new tools for gene regulatory analysis. *Nucleic Acids Res.*, **47**, D729–D735.
19. Hammal,F., de Langen,P., Bergon,A., Lopez,F. and Ballester,B. (2021) ReMap 2022: a database of human, mouse, drosophila and arabidopsis regulatory regions from an integrative analysis of DNA-binding sequencing experiments. *Nucleic Acids Res.*, **50**, D316–D325.
20. Kolmykov,S., Yevshin,I., Kulyashov,M., Sharipov,R., Kondrakhin,Y., Makeev,V.J., Kulakovskiy,I.V., Kel,A. and Kolpakov,F. (2021) GTRD: an integrated view of transcription regulation. *Nucleic Acids Res.*, **49**, D104–D111.
21. Li,R., Liang,F., Li,M., Zou,D., Sun,S., Zhao,Y., Zhao,W., Bao,Y., Xiao,J. and Zhang,Z. (2018) MethBank 3.0: a database of DNA methylomes across a variety of species. *Nucleic Acids Res.*, **46**, D288–D295.

22. Rhee,H.S. and Pugh,B.F. (2011) Comprehensive genome-wide protein-DNA interactions detected at single nucleotide resolution. *Cell*, **147**, 1408–1419.
23. Chereji,R.V., Bryson,T.D. and Henikoff,S. (2019) Quantitative MNase-seq accurately maps nucleosome occupancy levels. *Genome Biol.*, **20**, 198.
24. Wang,R., Yamada,T., Kita,K., Taniguchi,H., Arai,S., Fukuda,K., Terashima,M., Ishimura,A., Nishiyama,A., Tanimoto,A. *et al.* (2020) Transient IGF-1R inhibition combined with osimertinib eradicates AXL-low expressing EGFR mutated lung cancer. *Nat. Commun.*, **11**, 4607.
25. Groff,A.F., Barutcu,A.R., Lewandowski,J.P. and Rinn,J.L. (2018) Enhancers in the peril lincRNA locus regulate distant but not local genes. *Genome Biol.*, **19**, 219.
26. Hänsel-Hertsch,R., Simeone,A., Shea,A., Hui,W.W.I., Zyner,K.G., Marsico,G., Rueda,O.M., Bruna,A., Martin,A., Zhang,X. *et al.* (2020) Landscape of G-quadruplex DNA structural regions in breast cancer. *Nat. Genet.*, **52**, 878–883.
27. Roels,J., Kuchmiy,A., De Decker,M., Strubbe,S., Lavaert,M., Liang,K.L., Leclercq,G., Vandekerckhove,B., Van Nieuwerburgh,F., Van Vlierberghe,P. *et al.* (2020) Distinct and temporary-restricted epigenetic mechanisms regulate human αβ and γδ t cell development. *Nat. Immunol.*, **21**, 1280–1292.
28. Zou,Z., Iwata,M., Yamanishi,Y. and Oki,S. (2022) Epigenetic landscape of drug responses revealed through large-scale chip-seq data analyses. *BMC Bioinf.*, **23**, 51.
29. Tanaka,H., Igata,T., Etoh,K., Koga,T., Takebayashi,S.i. and Nakao,M. (2020) The NSD2/WHSC1/MMSET methyltransferase prevents cellular senescence-associated epigenomic remodeling. *Aging Cell*, **19**, e13173.
30. Ferris,E., Abegglen,L.M., Schiffman,J.D. and Gregg,C. (2018) Accelerated evolution in distinctive species reveals candidate elements for clinically relevant traits, including mutation and cancer resistance. *Cell Rep.*, **22**, 2742–2755.
31. Lizio,M., Abugessaisa,I., Noguchi,S., Kondo,A., Hasegawa,A., Hon,C.C., De Hoon,M., Severin,J., Oki,S., Hayashizaki,Y. *et al.* (2019) Update of the FANTOM web resource: expansion to provide additional transcriptome atlases. *Nucleic Acids Res.*, **47**, D752–D758.
32. Albrecht,F., List,M., Bock,C. and Lengauer,T. (2016) DeepBlue epigenomic data server: programmatic data retrieval and analysis of epigenome region sets. *Nucleic Acids Res.*, **44**, W581–W586.
33. Kehl,T., Schneider,L., Schmidt,F., Stöckel,D., Gerstner,N., Backes,C., Meese,E., Keller,A., Schulz,M.H. and Lenhof,H.P. (2017) RegulatorTrail: a web service for the identification of key transcriptional regulators. *Nucleic Acids Res.*, **45**, W146–W153.
34. Okuda,S., Watanabe,Y., Moriya,Y., Kawano,S., Yamamoto,T., Matsumoto,M., Takami,T., Kobayashi,D., Araki,N., Yoshizawa,A.C. *et al.* (2017) jPOSTrepo: an international standard data repository for proteomes. *Nucleic Acids Res.*, **45**, D1107–D1111.
35. Ochsner,S.A., Abraham,D., Martin,K., Ding,W., McOwiti,A., Kankanamge,W., Wang,Z., Andreano,K., Hamilton,R.A., Chen,Y. *et al.* (2019) The signaling pathways project, an integrated 'omics knowledgebase for mammalian cellular signaling pathways. *Scientific Data*, **6**, 252.
36. Kaya-Okur,H.S., Wu,S.J., Codomo,C.A., Pledger,E.S., Bryson,T.D., Henikoff,J.G., Ahmad,K. and Henikoff,S. (2019) CUT&Tag for efficient epigenomic profiling of small samples and single cells. *Nat. Commun.*, **10**, 1930.
37. Harada,A., Maehara,K., Handa,T., Arimura,Y., Nogami,J., Hayashi-Takanaka,Y., Shirahige,K., Kurumizaka,H., Kimura,H. and Ohkawa,Y. (2018) A chromatin integration labelling method enables epigenomic profiling with lower input. *Nat. Cell Biol.*, **21**, 287–296.
38. Lieberman-Aiden,E., Van Berkum,N.L., Williams,L., Imakaev,M., Ragoczy,T., Telling,A., Amit,I., Lajoie,B.R., Sabo,P.J., Dorschner,M.O. *et al.* (2009) Comprehensive mapping of long-range interactions reveals folding principles of the human genome. *Science*, **326**, 289–293.